Available online at www.sciencedirect.com

ScienceDirect

Geochimica et Cosmochimica Acta 188 (2016) 352–367

Geochimica et Cosmochimica Acta

www.elsevier.com/locate/gca

Evolution of chemical and isotopic composition of inorganic carbon in a complex semi-arid zone environment: Consequences for groundwater dating using radiocarbon

K.T. Meredith [a,*], L.F. Han [b], S.E. Hollins [a], D.I. Cendón [a], G.E. Jacobsen [a], A. Baker [c]

[a] *ANSTO, Nuclear Science and Technology – The Environment, New Illawarra Road, Lucas Heights, NSW 2234, Australia*
[b] *Hydrology and Water Resources Department, Nanjing Hydraulic Research Institute, Guangzhou Road 223, P.O. Box 210029, Nanjing, China*
[c] *Connected Waters Initiative Research Centre, University of New South Wales, Australia*

Received 9 November 2015; accepted in revised form 7 June 2016; available online 16 June 2016

Abstract

Estimating groundwater age is important for any groundwater resource assessment and radiocarbon (^{14}C) dating of dissolved inorganic carbon (DIC) can provide this information. In semi-arid zone (i.e. water-limited environments), there are a multitude of reasons why ^{14}C dating of groundwater and traditional correction models may not be directly transferable. Some include; (1) the complex hydrological responses of these systems that lead to a mixture of different ages in the aquifer(s), (2) the varied sources, origins and ages of organic matter in the unsaturated zone and (3) high evaporation rates. These all influence the evolution of DIC and are not easily accounted for in traditional correction models. In this study, we determined carbon isotope data for; DIC in water, carbonate minerals in the sediments, sediment organic matter, soil gas CO_2 from the unsaturated zone, and vegetation samples. The samples were collected after an extended drought, and again after a flood event, to capture the evolution of DIC after varying hydrological regimes. A graphical method (Han et al., 2012) was applied for interpretation of the carbon geochemical and isotopic data. Simple forward mass-balance modelling was carried out on key geochemical processes involving carbon and agreed well with observed data. High values of DIC and $\delta^{13}C_{DIC}$, and low $^{14}C_{DIC}$ could not be explained by a simple carbonate mineral–CO_2 gas dissolution process. Instead it is suggested that during extended drought, water–sediment interaction leads to ion exchange processes within the top ~10–20 m of the aquifer which promotes greater calcite dissolution in saline groundwater. This process was found to contribute more than half of the DIC, which is from a mostly 'dead' carbon source. DIC is also influenced by carbon exchange between DIC in water and carbonate minerals found in the top 2 m of the unsaturated zone. This process occurs because of repeated dissolution/precipitation of carbonate that is dependent on the water salinity driven by drought and periodic flooding conditions. This study shows that although ^{14}C cannot be directly applied as a dating tool in some circumstances, carbon geochemical/isotopic data can be useful in hydrological investigations related to identifying groundwater sources, mixing relations, recharge processes, geochemical evolution, and interaction with surface water.

Keywords: Radiocarbon; Carbon isotopes; Darling River; Groundwater; $CO_{2(g)}$; Unsaturated zone; Water–sediment reactions

* Corresponding author. Tel.: +61 2 9717 3155.
E-mail address: karina.meredith@ansto.gov.au (K.T. Meredith).

http://dx.doi.org/10.1016/j.gca.2016.06.011

1. INTRODUCTION

Estimating groundwater age is important for any groundwater resource assessment as it provides information on groundwater replenishment rates, recognises palaeowaters, and can be used to calibrate groundwater flow models, which ultimately offer guidance on the sustainability of a groundwater resource. Radiocarbon (^{14}C with a half-life of 5730 ± 40 years) provides a useful tool for estimating the age of groundwater recharged on the ten thousand year time scale. Most groundwater dating studies measure the ^{14}C contents of the dissolved inorganic carbon (DIC) and fundamental assumptions are made when calculating an age. In order to calculate radiocarbon age it is essential to estimate the initial ^{14}C content ($^{14}C_0$) and this has direct impact on the results. The calculation of a ^{14}C groundwater 'age' still has many hydrochemical and hydrogeological challenges associated with its use (Tamers, 1975; Fontes and Garnier, 1979; Maloszewski and Zuber, 1991; Sanford, 1997; Plummer and Sprinkle, 2001; Gonfiantini and Zuppi, 2003;, amongst many others).

The commonly used adjustment models for $^{14}C_0$ in radiocarbon dating of groundwater are based on simple conceptualisation of certain geochemical processes. For example, where the HCO_3^- in water is a reaction product of dissolved CO_2 and carbonate minerals under closed-system conditions, the Tamers' model can be used (Tamers, 1975; Han and Plummer, 2013, 2016). Where carbonate dissolution is occurring under open-system conditions while carbon exchange between DIC and CO_2 gas from the unsaturated zone occurs, Mook's model (Mook, 1976, 1980) can be applied. In scenarios where carbonate dissolution takes place partly under open-system conditions in the unsaturated zone and partly under closed-system conditions in the aquifer, the IAEA model can be applied (Salem et al., 1980; Gonfiantini and Zuppi, 2003; Han and Plummer, 2016). For combined processes of the above and carbon exchange between DIC and carbonate minerals, the Eichinger (Eichinger, 1983) or Han and Plummer (Han and Plummer, 2013) model can be used.

There are a multitude of reasons why these correction methods cannot be directly transferred to semi-arid or water-limited environments. Firstly, contrasting recharge mechanisms from direct (rainfall) and indirect (i.e. river water) will influence the evolution of DIC in groundwater. These environments generally experience very low direct recharge from rainfall because evaporation rates far outweigh precipitation. And in some cases river recharge can provide a greater overall volume of groundwater recharge, however these events may not be predictable, being delivered on multi-annual timescales dependent on flow regimes of dryland rivers such as the Darling River (Meredith et al., 2015). These conditions can lead to groundwater age gradients forming within an aquifer and promote the development of a thick unsaturated zone (Wood et al., 2014). Tracing the evolution of DIC in such complex hydrological systems is challenging.

Secondly, because many of the correction models calculate $^{14}C_0$ by using an assumed $\delta^{13}C$ value of CO_2 gas in the unsaturated zone, in water-limited environments, this value has been found to be more variable than first realised. Soil $CO_{2(g)}$ in the unsaturated zone can be contributed from shallow and deep sources with varying ages (Walvoord et al., 2005; Carmi et al., 2009). Wood et al. (2014) modelled soil $CO_{2(g)}$ by varying recharge rates and water table depth in a water-limited environment in Australia. They identified how these variables influenced shallow and deep productions of soil $CO_{2(g)}$ in a thick unsaturated zone (30 m). This study did not calibrate these models with sediment analysis, therefore, questions still remain as to the soil $CO_{2(g)}$ source and the associated geochemical processes leading to DIC evolution. Organic carbon can also be sourced from vegetation which utilises both the C_3 (trees) and C_4 (grasses) photosynthetic pathways (Plummer and Sprinkle, 2001; Plummer and Glynn, 2013). This organic matter maybe *in situ* (either root zone material or soil organic matter (SOM) (Carmi et al., 2009)). Or it may be dissolved or colloidal organic matter being transported within the unsaturated zone. In all cases, organic matter can undergo microbial reprocessing in the unsaturated zone (Shen et al., 2015; Mattey et al., 2016) leading to varying sources of $CO_{2(g)}$. Therefore, measuring this soil $CO_{2(g)}$ source is crucial for radiocarbon studies in water-limited environments.

Furthermore, the high evaporation rates experienced in these regions promote the formation of soil carbonates. This is because they form in soils with a net water deficit (Cerling and Quade, 1993). The carbonate forms when the solution becomes supersaturated with carbonate due to an increase in the concentration of dissolved ions. The presence of carbonate minerals is likely to further hinder the simplistic use of radiocarbon corrections in the Australian setting. Cartwright et al. (2013) showed the degree of closed-system calcite dissolution in groundwater that was recently recharged by using $^{14}C_{DIC}$ and ^{3}H. This dual isotope approach is useful for groundwaters that contain measureable ^{3}H and can be used to identify mixing trends.

Finally and most importantly for this study, the commonly used ^{14}C correction models imply conceptually that a water sample is unmixed and of a single age. Very often, a groundwater sample is composed of a mixture of waters with distinctly different ages especially where river waters are the major source of recharge. The influence of this mixing can be extreme, for example, a palaeowater with an age greater than 1 Ma can be mixed with 1% of modern water, it will then appear to be less than 30 ka giving misleading age information (Han and Plummer, 2016). Therefore identifying this mixing and the geochemical processes that are influenced by the influx of this water with a different chemistry is important and hence the subject of this research.

The aims of this paper are: (1) to test, with measured data of carbon chemical and isotopic composition of DIC, whether the commonly held assumptions for carbon evolution within both the unsaturated and saturated zones of a groundwater system in a semi-arid zone climate hold true; (2) to show that mixed water samples can be recognised by analysing the chemical and isotopic composition of DIC, and (3) to present a method for resolving the abovementioned issues associated with interpreting DIC data in a water limited environment and in doing so define

the contribution of DIC from river water mixing and water-sediment interaction processes.

2. STUDY AREA

The study area, known as Glen Villa, is located approximately 30 km southwest of Bourke along the Darling River (New South Wales, Australia; Fig. 1). The 250 km^2 site contains nested groundwater monitoring wells located adjacent to the Darling River (Meredith et al., 2009, 2013) which were measured after drought and again after a large river flood event (Meredith et al., 2015). The area has a semi-arid climate with low rainfall (average 397 mm yr^{-1}) and contains a narrow riverine corridor that runs along the Darling River. The river is a regulated system but flow is ultimately controlled by the climate within the wider Darling River catchment (Meredith et al., 2015).

The surficial geology comprises unconsolidated alluvial aquifers that have a similar sedimentology. These three aquifers are part of a closed and internally draining groundwater basin. The deeper aquifer is only found within a pre-Cenozoic palaeochannel that formed adjacent to the modern Darling River, within the underlying Great Artesian Basin. The other two aquifers are found throughout the site and both have average thicknesses of 30 m. The aquifer units are terrestrially sourced sediments that have originated from alluvial fan systems that were deposited in alternating wet/dry climates (Meredith et al., 2013). Sediments comprise clay and silts in the top 2 m and grade towards clay with sand (Meredith et al., 2015). A band of evaporite minerals containing gypsum and carbonaceous sediments occurs from 2 to 3 m depth where minerals precipitate after long periods of evaporation and partially dissolved after recharge events (Meredith et al., 2015). Local scale variability in sedimentology exists at the site. Based on drillers logs, the sediments were identified as being predominantly composed of clay-rich sediments, with the occasional discontinuous sand or gravel unit that were 1–3 m thick. Further geophysical exploration would be needed to identify the influence of these permeability contrasts on groundwater flow and inter-aquifer exchange at the site.

Groundwater recharge occurs mostly from overbank river recharge during flooding events. Water levels within the shallow (0–17 m bgs) aquifer close to the river responded to long-term (decadal) rainfall trends that are driven by high flow conditions in the river (Meredith et al., 2015). For example, during drought (i.e. June 2009), the unsaturated zone was a consistent depth ranging between 11 and 11.5 m below ground surface (bgs). Post-flooding of the Darling River (Jun 2012), the unsaturated zone depth near the river (<0.6 km) decreased to 6.7 m bgs and 10.1 m at 7 km from the river. A downward

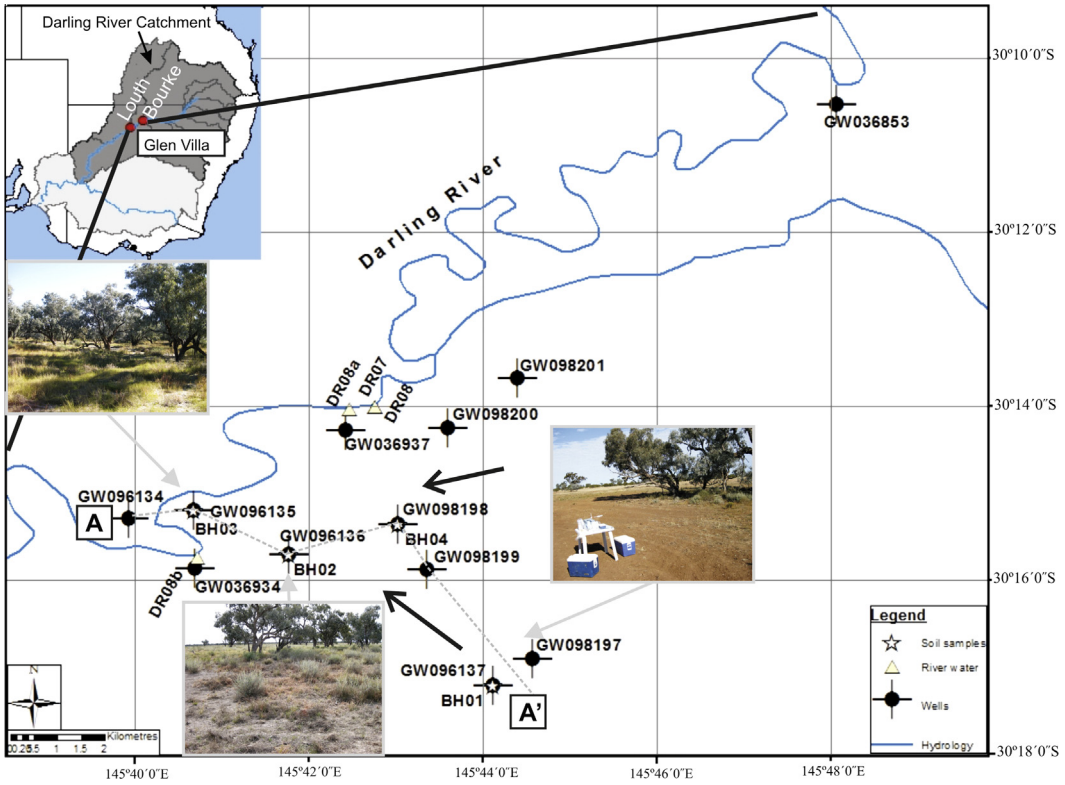

Fig. 1. Location of the Glen Villa study site (dashed lines show the location of cross section A-A′, Fig. 6) with reference to the limits of the Murray-Darling Basin (left top corner insert: light grey + dark grey extent) and the Darling River catchment (left top corner insert: dark grey extent). Locations of groundwater wells, soil/sediment (and soil gas) and river water sample locations are shown. Arrows show the generalised groundwater flow direction at the site during drought (August 2007) conditions. Photo inserts were taken in June 2012 to show the vegetation distribution at <0.6 km, 2.5 km and 7 km from the river.

hydraulic gradient was observed in the shallow water level indicating groundwater recharge from the river. Large flood events that exceed bank levels occurred approximately every 26 years with up to 40–60 mm of infiltration water across the site originating from the river (Meredith et al., 2015).

At distance from the river (>2.5 km) water levels generally showed an upward hydraulic gradient in the deeper sections (42–119 m bgs) of the aquifer suggesting limited downward flow from the shallow aquifer (Meredith et al., 2015). The dissimilarities in hydrochemistry of the groundwaters close to the river and at different depths with distance indicate waters have evolved along a different hydrochemical pathway and will be discussed in greater detail in this work. A carbon isotope data set was collected for DIC, carbonate minerals in the sediments, sediment organic matter (SOM), CO_2 gas from the unsaturated zone and vegetation samples. These were collected after drought to understand evaporation effects, and again after a large river flood event to understand recharge mechanisms. This was done to capture the DIC evolution after varying hydrological regimes which are expected to be consistent for semi-arid zone environments in the Australian setting.

3. METHODOLOGY

3.1. Field techniques

Water and sediment samples, were collected in June 2009 (drought) and all of these plus vegetation and CO_2 gas from the unsaturated zone were sampled in June 2012 (post-flood). Vegetation (leaf) samples from the dominant tree and grass species were collected in plastic zip lock bags from four locations in close proximity to the groundwater wells (see below). Five replicate samples (from different individual plants) were analysed for each vegetation type. At well location GW096135 (BH3; Fig. 1), two dominant grasses (unknown species) and one *Eucalyptus camaldulensis* (River Red Gum) was sampled. At well locations GW096136 (BH2), GW096137 (BH1) and GW098198 (BH4), one grass and one River Red Gum was sampled. These samples were then frozen.

Sediments were collected from boreholes (BH1-4) drilled throughout the unsaturated zone specifically to collect sediment samples in June 2009 during a dry period and again in June 2012 after a wet period. Sediment samples were collected off the auger using a motorised soil auger. Samples were collected from 0.5 m intervals into sealed glass jars. The CO_2 gas was sampled from three locations at BH1, BH2 and BH3 from 2 m and 5 m depths in June 12 (6 samples in total). Installation of gas samplers occurred after collection of sediment samples from the boreholes. See Wood et al. (2014) for extended description on design. The CO_2 gas was collected in pre-evacuated 110 ml Isotubes (with nitrogen gas) using a vacuum pump after three air volumes were removed.

River water samples were obtained from five locations (DR07, DR08, DR08a, DR08b and DR08c; Fig. 1) along the Darling River on May 2007, August 2007 and June 2012 according to the methods in Meredith et al., (2009). Groundwater samples were collected from nested monitoring wells on August 2007 and June 2009 (drought), and again in June 2012 (post-flood) (Fig. 1). After standing water levels were measured, the wells were purged of three well-volumes and until stabilisation of field parameters (electrical conductivity, oxidation–reduction potential, dissolved oxygen, temperature and pH) prior to sampling. Final readings of the parameters including pH were taken from an in-line flow cell. Water samples were collected from an in-line 0.45 μm polyethersulphone high capacity filter. Total alkalinity values were determined in the field by acid–base titration using a HACH digital titrator. Full details of the methodology for sample collection are provided in Meredith et al. (2012).

3.2. Analytical techniques

The $\delta^{13}C$ signatures of bulk vegetation (leaf) and sediment organic matter (SOM) samples were determined by elemental analyser/isotope ratio mass spectrometry (EA/IRMS). SOM samples were acidified, washed, dried and prepared according to the methods presented in Mazumder et al. (2010). Sediment samples were dried at 105 °C for 24 h then homogenised and crushed. Those that contained carbonate mineral(s) (as identified using X-ray Diffraction analysis and visual inspection during drilling) were determined for their bulk $\delta^{13}C_{CaCO3}$ signature and $^{14}C_{CaCO3}$ content.

The $\delta^{13}C$ signatures of carbonates, CO_2 gas from the unsaturated zone and waters were analysed by IRMS. Carbonates were reacted in evacuated Exetainer tubes with 104% phosphoric acid (H_3PO_4) at 25 °C overnight, prior to analysis. The CO_2 gas sub-samples were extracted using a gas syringe directly from the Isotubes that were used to collect the samples in the field. After injecting the CO_2 into a helium stream, which was separated from other gases by gas chromatography attached to a Finnigan 252 mass spectrometer using a Conflo III. Results were reported as per mil (‰) deviation from the international carbonate standard, NBS19 with a precision of ±0.1‰.

The DOC concentration and $\delta^{13}C_{DOC}$ were analysed using a total organic carbon analyser interfaced to a PDZ Europa20-20 IRMS utilising a GD-100 gas trap interface. Results were reported as per mil (‰) deviation from the NIST standard reference material with an analytical precision of ±0.6‰.

The ^3H activities were expressed in tritium units (TU) with varying uncertainties and quantification limits see Table 1. Generally, the 2007 and 2009 samples have an uncertainty of $\pm\leqslant 0.7$ TU and quantification limit of $\leqslant 0.3$ TU and 2012 samples have an uncertainty of $\pm\leqslant 0.1$ TU and quantification limit of $\leqslant 0.3$ TU. Samples were analysed by liquid scintillation counting. Extended methods for ^3H activities can be found in Meredith et al. (2012). The water samples were also analysed by ion chromatography for anions and inductively coupled plasma-atomic emission spectrometry for cations (Meredith et al., 2015) and charge balance errors (CBE) assessed (Table 1).

The ^{14}C content of waters ($^{14}C_{DIC}$), CO_2 gas from the unsaturated zone ($^{14}C_{CO2}$) and carbonates ($^{14}C_{CaCO3}$) were

Table 1
Hydrochemical and isotopic data for groundwaters. Depth = the mid-point between the top and bottom of the screen. DIC = dissolved inorganic carbon, S.I. calcite = saturation indices for calcite, Uncert. = ^{3}H uncertainty, QL = ^{3}H quantification limit, C.B.E = charge balance error for major ion data from Meredith et al., (2015).

ID Units	Date	Depth M	pH	$\delta^{13}C_{DIC}$ ‰	DIC mmol L^{-1}	CO_2 mmol L^{-1}	HCO_3^- mmol L^{-1}	$^{14}C_{DIC}$ pmc	^{3}H TU	Uncert. TU	QL TU	Na mmol L^{-1}	Cl mmol L^{-1}	Ca mmol L^{-1}	$SI_{Calcite}$	C.B.E. %
GW036853/1	25/08/2007	16	6.66	−15.3	4.8	1.5	3.3	126.2	2.1	0.7	0.3	2.9	2.5	0.9	−1.0	−4.9
GW036853/2	24/08/2007	43	6.32	−8.8	6.9	2.4	3.5	3.0	0.2	0.7	0.3	244.0	341.3	26.4	−0.3	−1.9
GW036853/3	25/08/2007	126	6.41	−7.8	9.0	2.5	4.8	9.9	0.1	0.7	0.3	321.4	431.6	30.2	−0.1	−0.4
GW036934/1	23/08/2007	13	6.29	−13.0	2.7	1.3	1.3		0.4	0.3	0.3	4.7	7.4	1.3	−1.6	1.8
GW036934/1	25/06/2009	13	6.31	−14.2	2.8	1.4	1.4	92.8	0.4	0.3	0.3	6.4	9.9	1.5	−1.5	−2.0
GW036934/2	23/08/2007	39	6.38	−8.4	9.1	2.8	4.8	27.7	0.1	0.5	0.3	357.1	479.5	24.4	−0.2	−5.8
GW036934/2	24/06/2012	39	6.60	−10.9	7.8	1.7	4.8	25.5	0.32	0.03	0.13	339.7	400.5	22.0	−0.1	−1.0
GW036934/3	23/08/2007	72	6.41	−8.5	9.1	2.6	4.9	21.9	0.1	0.3	0.3	364.5	456.9	24.0	−0.2	−2.9
GW036934/3	24/06/2012	72	6.59	−11.5	9.0	1.9	5.3	33.0	0.13	0.03	0.14	389.3	442.8	24.4	0.0	0.2
GW036937/1	23/08/2007	17	6.54	−11.8	5.8	1.8	3.6	84.5	0.3	0.3	0.3	57.9	78.7	5.1	−0.6	−5
GW036937/1	22/06/2012	17	6.65	−13.6	6.5	1.7	4.4	89.6	0.50	0.04	0.14	63.1	79.8	6.0	−0.4	−1.6
GW036937/2	24/08/2007	43	6.44	−7.6	8.0	2.2	4.4	18.2	0.1	0.3	0.3	307.1	389.3	26.7	−0.1	0.2
GW036937/2	22/06/2012	43	6.57	−9.6	7.7	1.7	4.6	17.8	0.13	0.03	0.14	312.7	394.9	27.4	0.0	−1.0
GW036937/3	23/08/2007	110	6.37	−8.4	11.5	3.3	6.0	39.7	0.1	0.4	0.3	371.9	490.8	31.9	0.0	−1.7
GW036937/3	23/06/2012	110	6.56	−10.6	9.4	2.0	5.4	40.1	0.27	0.03	0.15	399.3	479.5	32.9	0.2	0.8
GW096134/1	25/08/2007	32	6.41	−10.3	6.6	1.7	3.3	28.0	0.2	0.7	0.3	372.3	578.2	50.2	0.0	−2.4
GW096135/1	24/08/2007	16	6.41	−9.4	11.2	3.4	6.1	82.2	0.1	0.3	0.3	274.9	462.6	27.7	0.0	−12.1
GW096135/1	20/06/2012	16	6.53	−13.5	4.3	1.4	2.7	96.8	1.42	0.07	0.14	49.6	66.6	5.4	−0.7	−1.6
GW096135/2	24/08/2007	28	6.36	−9.0	8.8	2.7	4.5	31.4	0.3	0.7	0.3	350.2	479.5	33.2	−0.1	−2.2
GW096135/2	20/06/2012	28	6.46	−11.8	7.8	2.1	4.3	37.3	0.29	0.03	0.14	313.2	411.8	31.4	−0.1	−0.8
GW096135/3	24/08/2007	42	6.35	−9.3	8.9	2.7	4.6	30.6	0.1	0.3	0.3	347.1	485.2	30.4	−0.2	−4.3
GW096135/3	20/06/2012	42	6.60	−12.4	6.6	1.5	4.1	48.3	1.27	0.06	0.14	226.6	293.3	21.0	−0.1	−1.9
GW096136/1	21/08/2007	17	6.41	−9.5	7.8	2.3	4.2	74.9	0.5	0.3	0.3	340.6	428.7	29.7	−0.2	0.9
GW096136/1	22/06/2012	17	6.51	−10.9	8.3	2.1	4.7	71.2	0.19	0.02	0.12	335.4	437.2	28.7	0.0	−2.7
GW096136/2	22/08/2007	37	6.24	−9.1	10.0	3.6	4.6	68.7	0.1	0.3	0.3	357.5	496.4	33.2	−0.2	−3.1
GW096136/2	22/06/2012	37	6.41	−11.5	9.9	2.8	5.2	69.1	0.10	0.02	0.12	371.9	468.2	33.7	0.0	−0.1
GW096136/3	21/08/2007	119	6.4	−9.0	9.2	2.7	5.0	9.5	0.1	0.5	0.3	365.4	454.1	21.8	−0.3	−3.2
GW096136/3	22/06/2012	119	6.52	−10.9	8.5	2.0	4.9	9.4	0.08	0.02	0.12	376.7	437.2	22.6	−0.1	−1.3
GW096137/1	22/08/2007	15	6.74	−5.6	11.4	1.8	7.3	60.6	0.1	0.3	0.3	411.9	456.9	17.8	0.1	−1.8
GW096137/1	21/06/2012	15	6.96	−8.9	11.2	1.2	7.8	65.6	0.02	0.06	0.37	425.0	462.6	18.2	0.4	−2.8
GW096137/2	22/08/2007	22	6.55	−5.8	14.7	3.2	8.6	62.6	0.1	0.4	0.3	431.9	473.9	18.8	0.1	−1.2
GW096137/2	21/06/2012	22	6.70	−8.7	10.6	1.8	6.7	62.9	0.25	0.03	0.12	448.0	479.5	18.7	0.1	−2.1
GW096137/3	22/08/2007	52	6.57	−9.9	8.3	2.0	5.2	0.8	0.1	0.3	0.3	272.7	310.3	11.2	−0.3	−1.2
GW096137/3	21/06/2012	52	6.70	−11.0	7.8	1.5	5.2	0.8	0.27	0.03	0.12	275.3	304.6	11.4	−0.2	−0.9
GW098197/1	23/06/2009	41	6.61	−9.8	9.1	1.8	5.5	43.1	0.1	0.3	0.3	504.6	535.9	18.7	−0.1	−2.8
GW098197/2	23/06/2009	56	6.63	−8.9	8.9	1.7	5.5	54.5	0.1	0.3	0.3	508.9	564.1	18.3	−0.1	−5.1
GW098198	24/06/2009	12	6.69	−10.2	5.6	1.0	3.5	67.6	0.2	0.3	0.3	326.7	507.7	29.7	0.0	−9.6
GW098198	23/06/2012	12	6.77	−9.7	5.6	0.9	3.5	68.3	0.24	0.03	0.13	347.5	462.6	32.4	0.1	−2.1
GW098199/1	24/06/2009	22	6.62	−9.9	7.9	1.7	4.8	55.5	0.1	0.3	0.3	325.8	479.5	27.7	0.0	−7.8
GW098199/2	24/06/2009	102	6.48	−10.7	9.8	2.5	5.5	40.2	0.3	0.3	0.3	374.5	535.9	27.9	0.0	−8.7
GW098200	25/06/2009	14	6.42	−11.3	13.2	3.7	7.2	103.8	0.4	0.3	0.3	345.8	535.9	32.9	0.1	−9.4
GW098201	25/06/2009	96	6.61	−10.1	7.3	1.6	4.5	20.2	0.1	0.3	0.3	282.3	394.9	23.2	0.0	−6.0

determined by accelerator mass spectrometry after samples were processed according to the methods outlined in Meredith et al. (2012), Wood et al. (2014) and Hua et al. (2001), respectively. Briefly, the total DIC or carbonate was processed into CO_2 by acidifying the samples and extracting the liberated CO_2 gas. The CO_2 gas from the unsaturated zone was extracted using a gas syringe directly from the Isotube. The CO_2 sample was then heated with CuO, Ag and Cu wire, at 600 °C for 2 h and then converted into graphite by reducing it with excess hydrogen gas in the presence of an iron catalyst at 600 °C.

The ^{14}C results reported from the laboratory were in percent Modern Carbon (pMC) normalised against the $\delta^{13}C$ of the graphite, with an average 1σ error of the AMS readings at ±0.3 pMC. We use the 'un-normalised' ^{14}C values for groundwater and report them as pmc which was calculated using the $^{14}C/^{12}C$ ratio (Plummer and Glynn, 2013). We do this because in groundwater the variation in $\delta^{13}C$ of DIC is caused by geochemical reactions that may affect $\delta^{13}C_{DIC}$ and $^{14}C_{DIC}$ differently. For example, carbon exchange between DIC and solid carbonate in the aquifer may cause an increase in $\delta^{13}C_{DIC}$ and a decrease in $^{14}C_{DIC}$. On the contrary, carbon exchange between DIC and soil CO_2 may cause a decrease in $\delta^{13}C_{DIC}$ and an increase in $^{14}C_{DIC}$. For this reason, normalisation of the $^{14}C_{DIC}$ value against the graphite value would introduce additional error into the age calculations.

3.3. Hydrogeochemical interpretation and modelling

Saturation indices (calcite), concentration of dissolved inorganic carbon [DIC], carbon dioxide [CO_2], carbonate [CO_3^{2-}] and bicarbonate [HCO_3^-] were calculated using the WATEQ4F thermodynamic database in the PHREEQC 3.1.7 programme (Parkhurst and Appelo, 1999). PHREEQC 3.1.7 programme was also used to model the distribution of carbon isotopes between the water and calcite. We use the graphical method developed by Han et al. (2012) to interpret groundwater evolution based on the concentration and the isotopic composition of the DIC. The method is described in detail in Section 5.2.

4. RESULTS

4.1. Vegetation

The vegetation distribution is shown in photos from the field site (Fig. 1). The riverine corridor located close to the river at BH03 contains the greatest number of River Red Gums with a grassy understorey vegetation distribution. The average $\delta^{13}C$ values of River Red Gum leaf samples at this site are −30.1‰ ($n = 5$) and −13.2‰ ($n = 10$) for grasses. These values are within the expected C_3 values for trees and C_4 for grasses which is reflected in all tree and grass results from the study site. At BH02 the trees become fewer with average $\delta^{13}C$ values of −28.6‰ ($n = 5$) and grass cover with average $\delta^{13}C$ values of −13.9‰ ($n = 3$) dominate the distribution. This is similar for 3 km (BH04) from the river with trees that have an average $\delta^{13}C$ values of −29.0‰ ($n = 5$). The site located the greatest distance from the river (7 km) contains the occasional tree with average $\delta^{13}C$ values of −27.3‰ ($n = 5$) at 7 km (BH01) and sparse grass cover with average $\delta^{13}C$ values of −14.6‰ ($n = 5$).

4.2. Sediment organic matter (SOM)

The SOM contents were highest in the surface sediments (BH03: 2.0%) (Fig. 2a) and decreased to less than 0.2% at 2 m bgs. These profiles do not contain significant amounts of organic matter compared to temperate environments and the reasons for this will be discussed in greater detail below. The borehole located closest to the river (<0.6 km) had a C_3 signature throughout the depth profile (to 5 m) with an average $\delta^{13}C$ value of −23.7‰ ($n = 11$) (Fig. 2b). The depth profile in the boreholes >2.5 km from the river showed a C_4 signature in the top 2.5–3 m shifting to C_3 signature beneath this depth (Fig. 2b). This shift indicates a change in organic matter source(s) with depth and distance from the river.

4.3. Carbonate minerals in the unsaturated zone

The $\delta^{13}C$ values of carbonate minerals from dry and wet periods ($\delta^{13}C_{CaCO3}$) ranged from −11.3‰ to -7.8‰. The sediment profile located 2.5 km from the river generally had lower $\delta^{13}C$ values (average value of −10.5‰, $n = 5$) than those in the profile located 7 km from the river, which have an average value of −9.6‰ ($n = 8$) in the top 2 m and even more enriched values at 5 m bgs (−7.8‰) (Fig. 2c). Carbon isotopic compositions of the carbonate minerals changed between dry and wet periods. Post-flooding (wet), the $\delta^{13}C_{CaCO3}$ values were generally more depleted, and at 1.5 m and 5 m were ~1‰ more depleted (Fig. 2c). This change was also observed in the ^{14}C of carbonates ($^{14}C_{CaCO3}$) values (Fig. 2d). At 0.5 m depth, the values were consistent ranging from 87.0 to 86.2 pMC but at 1 m and 1.5 m depth they increased from 71.0 to 83.1 and 44.1 to 51.5 pMC. This increase in $^{14}C_{CaCO3}$ shows that carbon exchange is influencing these sediments and will be discussed in greater detail below. At 5 m depth, there was only a slight decrease from 1.9 to 1.3 pMC.

4.4. The CO_2 gas from the unsaturated zone

The $\delta^{13}C$ values of CO_2 gas ($\delta^{13}C_{CO2}$) from the unsaturated zone at 2 and 5 m depth along the 7 km transect were relatively consistent (−21.5% to −22.7‰, Fig. 2b) with an average value −22.0‰ ($n = 5$) and were above 102 pMC for $^{14}C_{CO2}$ ($n = 3$). The CO_2 concentration was not measured in this study. The depth and distance from the river did not influence the ^{14}C value. These results suggest that CO_2 gas in the unsaturated zone is modern and is contributed from vegetation that has undergone the C_3 photosynthetic pathway either from organic matter degradation in the soil profile or from root zone respiration. It is not possible to differentiate these sources in this study (and nor was it the original purpose) because both processes will produce similar ^{14}C and ^{13}C values. Interestingly when we look at the extremely low SOM values (<0.2%) in the soil

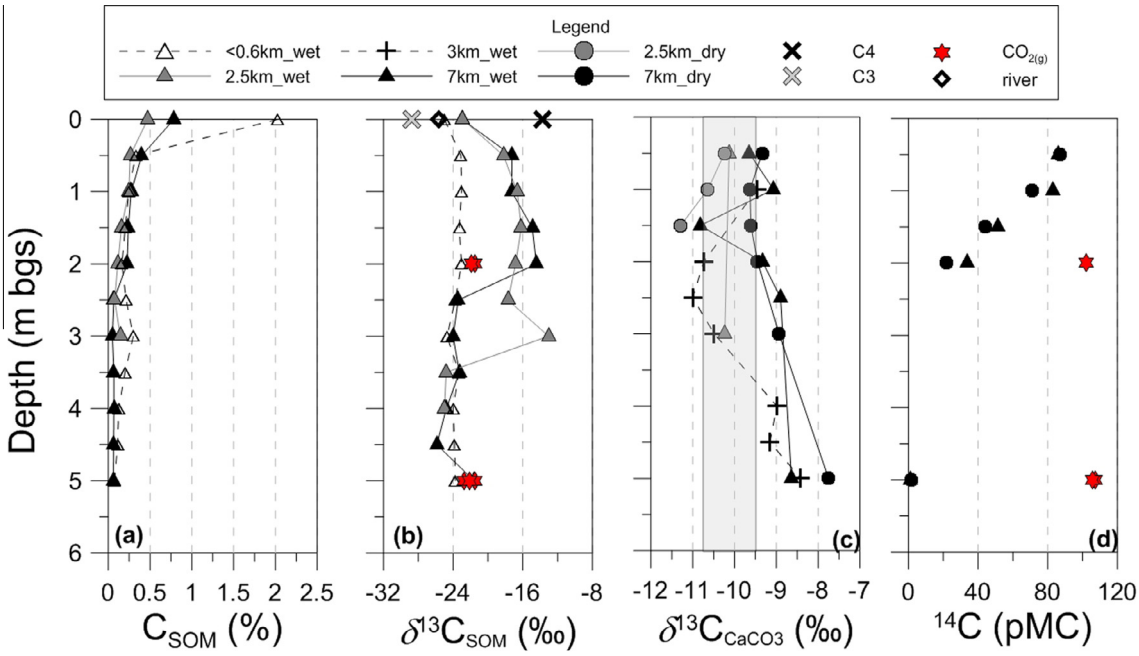

Fig. 2. Depth distribution plots through the top 5 m of the unsaturated zone at <0.6 km (BH03), 2.5 km (BH02), 3 km (BH04) and 7 km (BH01) from the river for (a) total carbon concentration of sediment organic matter post-flood sampling event in June 12 (wet), (b) $\delta^{13}C$ of sediment organic matter, $CO_{2(g)}$ in the unsaturated zone, and average C_3 and C_4 vegetation from the post-flood sampling event, (c) $\delta^{13}C_{CaCO3}$ of the carbonate minerals from drought in June 2009 and post-flood sampling events with the modelled calcite mineral range depicted by grey shaded rectangle calculated based on a measured $CO_{2(g)}$ value of −22.0‰ (see methods) and (d) ^{14}C (pMC) for carbonate minerals from BH01 located 7 km from the river sampled after drought and post-flood events with $CO_{2(g)}$ from the unsaturated zone.

profile, we can assume that organic matter contribution from surface vegetation and SOM is low. This will be discussed in detail in Section 5.1.

4.5. Water

The $\delta^{13}C_{DIC}$ values of river water ranged from −6.5‰ to −10.0‰ with an average of −8.6‰ ($n = 11$). The pH values range from 7.9 to 8.2. The river water contained less DIC than groundwater (i.e. average [DIC] = 2.7 mmol L^{-1}; $n = 13$) and an initial average DOC concentration of 7.2 mg L^{-1} ($n = 9$) with an average $\delta^{13}C_{DOC}$ value of −25.6‰ ($n = 8$). These $\delta^{13}C_{DOC}$ values are slightly lower than those measured in the Murray River ranging from −21‰ to −24‰ (Cartwright, 2010). We see that the DOC in the fresh groundwater close to the river sampled after the flood event (June 2012) was slightly more depleted in ^{13}C with an average $\delta^{13}C_{DOC}$ value of −27.4‰ ($n = 2$) and had slightly lower DOC concentration of 5 mg L^{-1} than the river water.

Groundwaters were mildly acidic (average pH of 6.52; $n = 43$). DIC concentrations were most varied in the shallow aquifer; with fresher (dilute) groundwater close to the river being the lowest concentration (4.3 mmol L^{-1}), pH of 6.53 and under-saturated with respect to calcite (−0.7). Groundwater furthest from the river have the highest concentrations (14.7 mmol L^{-1}), pH of 6.55 and are in equilibrium with respect to calcite (0.1) (Fig. 3a, Table 1).

Shallow dilute groundwaters close to the river channel (<0.6 km) were more depleted in ^{13}C ($\delta^{13}C_{DIC}$ ranged from −15.3‰ to −11.7‰) than those located 7 km ($\delta^{13}C_{DIC}$ ranged from −5.4‰ to −9.8‰) (Fig. 3b). The $^{14}C_{DIC}$ values decrease with depth but no obvious relationship was observed with distance from the river channel (Fig. 3c).

Distinct variations between dry and wet periods were observed, for example, the shallow groundwater located close to the river (GW096135/1), decreased in concentration of DIC from 11.2 mmol L^{-1} in the dry period to 4.9 mmol L^{-1} in the wet with a corresponding depletion in ^{13}C ($\delta^{13}C_{DIC}$ from −9.4‰ to −13.5‰) and increase in $^{14}C_{DIC}$ (82.2–96.8 pmc). Tritium values also increased after the wet period from 0.1 to 1.4 TU. The estimated rainfall weighted ^{3}H in Australian rainfall for 2005–2011 ranges from 2.4 to 2.8 TU for the area (Tadros et al., 2014) providing further evidence of modern river recharge into the shallow aquifer (Meredith et al., 2015).

The variation in carbon (but not to the same magnitude) was also observed at 7 km from the river (GW096137/1) with a fairly constant [DIC] but decreased in $\delta^{13}C_{DIC}$ (from −5.6‰ to −8.9‰) and increased in $^{14}C_{DIC}$ (from 60.8 to 65.4 pmc). Tritium values did not change after this event at 7 km from the river (Table 1).

5. DISCUSSION

5.1. Carbon sources in the unsaturated zone

Organic carbon in the unsaturated zone may originate from many sources (Allison et al., 2010; Longnecker and Kujawinski, 2011) but at this study site it is likely to be

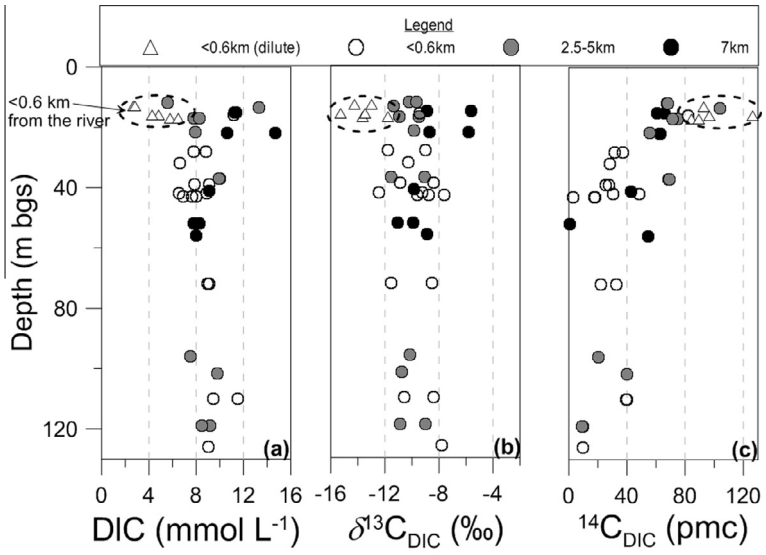

Fig. 3. Depth distribution plots of all groundwaters sampled with dilute groundwaters (<0.6 km from the river) highlighted by the dotted oval (a) DIC concentration (b) $\delta^{13}C_{DIC}$ and (c) $^{14}C_{DIC}$. Note 'dilute' is shallow (less than 20 m in depth) groundwater that has mixed with river water.

from either the degradation of (1) *in situ* organic matter and/or from (2) riverine input transported from flood events. The riparian corridor has the greatest biomass concentration for the area dominated by River Red Gums but their abundance decreases with distance from the river, with C_4 grasses becoming dominant at BH01 (Fig. 1; see photo insert). The vegetation cover is much less than what is observed in temperate environments and is reflected in the SOM content of the unsaturated zone with generally low total organic carbon percentages (<0.5%; Fig. 2a). The reasons for this are that in water-limited environments, such as this, rainfall is low and temperatures are high leading to low rates of biomass accumulation at the land surface. The SOM in the unsaturated zone is not being replaced by newly produced plant-derived sediment carbon (Quinton et al., 2010) as what is seen in temperate climates suggesting that *in situ* organic matter accumulation may be limited.

An alternative carbon source could be organic matter transported via river flood events that inundate and infiltrate into the unsaturated zone, where it is then subjected to microbial reprocessing (Shen et al., 2015). These floodwaters would also control the supply of fresh carbon required to stimulate microbial degradation (Fontaine et al., 2007) of existing SOM in the unsaturated zone. The microbial biomass and extracellular enzymes would then catalyse the conversion of polymeric sediment organic carbon to DOC (Allison et al., 2010). River water has a relatively high DOC concentration (average [DOC] $= 7.2\ mg\ L^{-1}$; $n = 9$) and a C_3 signature (average $\delta^{13}C_{DOC} = -25.6‰$; $n = 8$), similar to the recently recharged groundwater ([DOC] $= 5\ mg\ L^{-1}$ and average $\delta^{13}C_{DOC} = -27.4‰$: $n = 2$) suggesting a riverine source for the recently recharged groundwater. This is supported by the observation of groundwater recharge from river water after overbank flooding (Meredith et al., 2015).

Whether the SOM is transported or has formed *in situ*, the $\delta^{13}C_{SOM}$ signatures in the unsaturated zone located close to the river reflect a dominant C_3 organic matter source (Fig. 2b) similar to the vegetation (River Red Gums) and the DOC (river and groundwater). The $CO_{2(g)}$ values of the unsaturated zone with an average $\delta^{13}C_{CO2}$ value of −22‰ ($n = 5$) also suggests a C_3 organic matter source where organic matter had a starting value of ca. −26‰ (considering the fractionation of $CO_{2(g)}$ due to diffusion is ca. 4‰; (Cerling et al., 1991)). The $CO_{2(g)}$ in the top 5 m of the unsaturated zone was also found to be modern with ^{14}C values greater than 102 pMC ($n = 3$). These findings suggest soil $CO_{2(g)}$ is from a recent source assimilated from the atmosphere by plants with a C_3 signature via photosynthesis either from root respiration or decomposition of young organic matter (Carmi et al., 2009).

A consistent C_3 signature is observed near the river but a clear transition from C_3 to C_4 vegetation is evident in the SOM profiles located with distance from the river (i.e. >2.5 km; Fig. 2b). It is not until deeper in the unsaturated zone (Fig. 2b; 3.5 m) that the C_3 signature is seen. This means that the shallower parts of the unsaturated zone (0.5–3 m) are influenced by SOM from the C_4 grasses which are representative of the current land surface vegetation distribution (Fig. 1 refer to photo inserts from BH02 and BH01) or river water. Interestingly, the C_4 organic matter signal is not reflected in the $CO_{2(g)}$ values at 2 m depth (Fig. 2b) suggesting that the degradation of the *in situ* C_4 SOM is not the dominant source of $CO_{2(g)}$. This difference between SOM and soil gas can be explained by the influx of $CO_{2(g)}$ from microbial degradation or from organic matter respiration such as from tree roots in this part of the unsaturated zone. Carmi et al. (2013) found that 70–80% of soil $CO_{2(g)}$ was attributed to biotic processes which included root respiration even in an semi-arid zone environment with

limited vegetation cover. Amundson et al. (1994) also found that 50% of the soil $CO_{2(g)}$ was from root respiration. The difference between the SOM signature and soil $CO_{2(g)}$ is only evident in one location and the SOM signature returns to C_3 SOM with depth (Fig. 2b). Because root zone respiration and microbial degradation are both modern processes, deconvoluting their contribution to the soil $CO_{2(g)}$ of the unsaturated zone cannot be determined with this dataset.

It was not the main objective of this study to determine the source of SOM or soil $CO_{2(g)}$ in the unsaturated zone but rather to provide indication of their initial signature source. Importantly, we can rule out that CO_2 gas in the unsaturated zone has originated from a C_4 vegetation source. This finding is significant for any groundwater study that uses radiocarbon dating because it provides data which is generally assumed (for example see mass balance calculations i.e. Eqs. (1)–(3) below). We also show that the oxidation of fossil organic material is not a significant source of 'dead' carbon for infiltrating groundwater recharge within these alluvial sediments because the formation of $CO_{2(g)}$ in the unsaturated zone is a modern process. Other studies in water-limited environments containing far deeper unsaturated zones (30–110 m) than what was observed in our study site (i.e. less than 12 m depth) had soil gas CO_2 values which were less than 70 pMC (Walvoord et al., 2005; Wood et al., 2014). These low values were attributed to being diluted by an 'old' source of CO_2 from either organic or inorganic processes. The modern source in this study further supports the influx of $CO_{2(g)}$ from microbial degradation or from tree root respiration in the unsaturated zone.

Terrestrial carbonate minerals were not identified visually or by X-ray Diffraction analysis in sediments close to the river (<0.6 km) but were in profiles that were located a greater distance from the river (>2.5 km). Salinity increases were also observed in sediments which were found to be associated with river water flooding and evaporation cycles over-time (Meredith et al., 2015). Soils located the greatest distance from the river (7 km) have higher contents of carbonates because higher water deficits exist. The $\delta^{13}C$ and ^{14}C content of carbonates is controlled by soil $CO_{2(g)}$ (Cerling and Quade, 1993; Amundson et al., 1994). Therefore, using the measured $\delta^{13}C$ values of $CO_{2(g)}$ from the unsaturated zone, we calculate the expected $\delta^{13}C$ of a carbonate (Appelo and Postma, 2005). The shaded grey rectangle shows carbonates from the top 3 m are more likely to have formed from CO_2 gas that originated from C_3 plants (Fig. 2c).

Continuous profiles $\delta^{13}C$ of the carbonate minerals were not measured due to the patchy distribution of carbonate minerals but where carbonates did occur differences between dry and wet periods were observed at 1.5 m and 5 m (ca 1‰ more depleted; Fig. 2c). This change was more obvious for the $^{14}C_{CaCO3}$ values (Fig. 2d), where a 12 pMC increase was observed at 1 m depth after groundwater recharge. Importantly for this study is that these measurements show that there is intensive and/or fast carbon exchange between DIC in water and solid carbonate reaching down to five metres in the unsaturated zone and that it is driven by drought/flood conditions (further description is provided below). The shallow soil profiles located >2.5 km from the river contain a significant amount of 'dead' carbon which is expected to influence the evolution of DIC in the unsaturated zone.

5.2. Evolution of DIC

In most groundwater studies, radiocarbon dating of groundwater depends on the measured ^{14}C content of DIC. In the course of evolution of DIC starting from soil gas CO_2 in the unsaturated zone, many geochemical processes may change the carbon isotopic composition of DIC ($^{14}C_{DIC}$ and $\delta^{13}C_{DIC}$), by means of addition, removal, mixing, and exchange of carbon isotopes. The carbon isotopic composition of DIC and the concentration of DIC ([DIC]) is thus a result of many physical/geochemical processes involving different carbon-bearing sources that may have different carbon isotopic compositions (Han et al., 2012).

Identifying the carbon-bearing sources and the processes involved in the evolution of DIC in groundwater is essential in interpretation of ^{14}C data. Forward and backward hydrochemical modelling techniques can be used to obtain this information (Plummer, 1977; Wigley et al., 1978; Parkhurst and Appelo, 1999; Plummer and Glynn, 2013). Graphical methods such as the one developed by Han et al. (2012) also provide another means of analysing the geochemical/isotopic data for possible carbon-bearing sources and geochemical processes involved in the evolution of DIC.

Using the above mentioned graphical method, the critical points are first plotted in three sub-diagrams with the coordinates of $\delta^{13}C_{DIC}$ vs. 1/[DIC] (sub-diagram I), $^{14}C_{DIC}$ vs.1/[DIC] (sub-diagram II), and $^{14}C_{DIC}$ vs. $\delta^{13}C_{DIC}$ (sub-diagram III), respectively. Each critical point represents a carbon source (e.g. soil CO_2, solid carbonate, geogenic CO_2, CO_2 from decomposition of fossil organic matter), with defined values of concentration and carbon isotopic composition (e.g. Fig. 4). The measured sample data are then projected on these diagrams (e.g. symbols in Fig. 4) and their relations with the critical points are analysed with the help of process lines (e.g. the arrow lines in Fig. 4).

It is generally accepted that the process of ^{14}C decay will cause a decrease in $^{14}C_{DIC}$ in a groundwater system, without causing measurable change in the $\delta^{13}C_{DIC}$ and/or [DIC]. Most geochemical processes, however, would cause not only changes in $^{14}C_{DIC}$ but also in $\delta^{13}C_{DIC}$ and/or [DIC] (Han and Plummer, 2016). For example, carbonate dissolution by dissolved soil CO_2 under closed-system conditions would cause the $^{14}C_{DIC}$ and $\delta^{13}C_{DIC}$ values to change towards the values of the solid carbonate (generally a decrease in $^{14}C_{DIC}$, and conversely an increase in $\delta^{13}C_{DIC}$, and an increase in [DIC]). Another example is carbon exchange between DIC and soil CO_2 under open-system conditions. This process would cause the $^{14}C_{DIC}$ and $\delta^{13}C_{DIC}$ values to change towards the values of the soil CO_2 (generally an increase in $^{14}C_{DIC}$, a decrease in $\delta^{13}C_{DIC}$, and not affect [DIC]. In contrast, carbon exchange between DIC and solid carbonate in the aquifer under closed-system conditions would generally cause a decrease in $^{14}C_{DIC}$, an

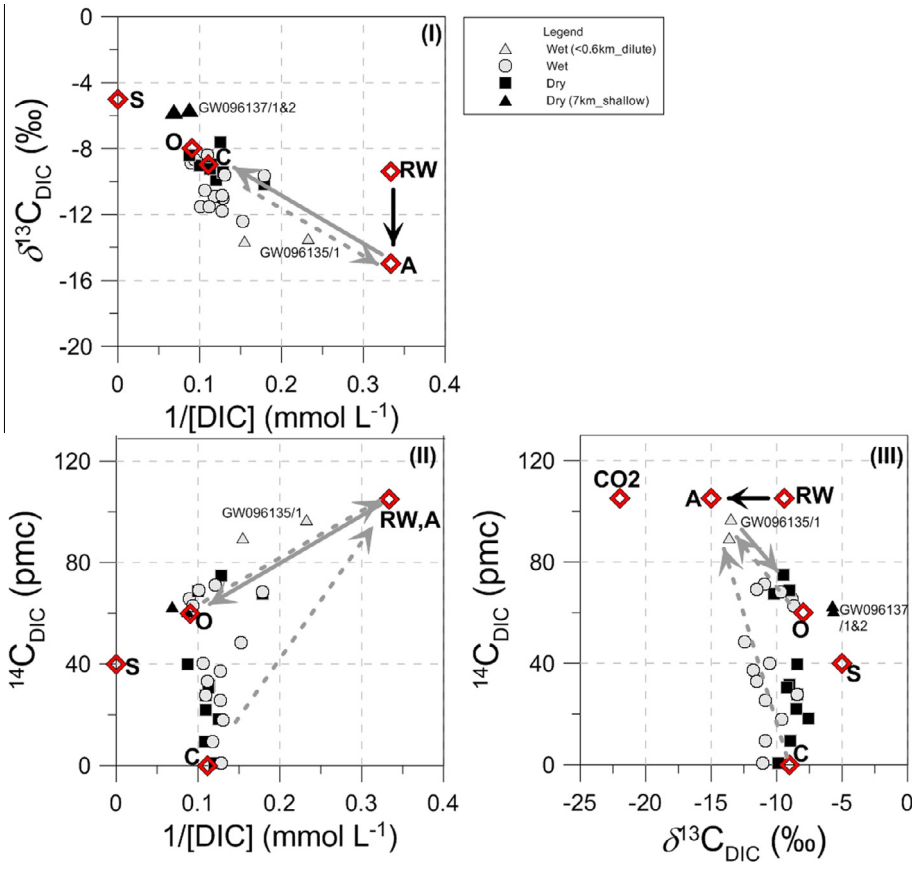

Fig. 4. The $^{14}C_{DIC}$–$\delta^{13}C_{DIC}$–[DIC] diagrams (Han and Plummer diagrams; Han and Plummer, 2013) of the data for samples collected after a drought period (dry: August 2007 and June 2009) and collected post-flood event (wet: June 2012). See text for explanation of carbon sources (RW, S), end members of geochemical evolution (A, O and C), and processes.

increase in $\delta^{13}C_{DIC}$, and little effect on [DIC]. Therefore, by using the graphical method, some common simple geochemical processes that affect the $^{14}C_{DIC}$ in aquifers can be identified, based on constraints of carbon isotopic compositions ($^{14}C_{DIC}$ and $\delta^{13}C_{DIC}$) and [DIC]. More information and examples on data interpretation using the graphical method are presented in Han et al. (2012) and Han and Plummer (2016).

In Fig. 4, river water (RW) is the known carbon-bearing input water source. The RW value was chosen after high flow events (June 2012) which are more representative of waters that are likely to recharge the aquifer. The river water, with $\delta^{13}C_{DIC}$ signatures of -9.4 ± 0.1‰ and [DIC] of 3 ± 0.1 mmol L^{-1} (Table 2) reflects in-river processes rather than groundwater influx which can influence the river water chemistry during drought (Meredith et al., 2009). Direct rainfall onto the catchment at the same time as river flooding could also influence the chemistry of the river recharge. However, after a thorough assessment of rainfall and river water time-series using the ^{18}O and ^{2}H values, it was found that groundwater is of flood water origin (Meredith et al., 2015) and not rainfall. Therefore, based on the measured values of RW, $CO_{2(g)}$ in the unsaturated zone and groundwater samples, three groundwater end-members were delineated, represented by letters A, O and C (Table 2, empty diamonds in Fig. 4). The hydrochemical evolutions of these end-members are discussed in detail below.

Table 2
Carbon sources and end-members of geochemical evolution.

Substance	$\delta^{13}C$	^{14}C content	DIC
Units	‰	pmc	mmol L^{-1}
DIC (river water)	−9.4	105	3
Soil CO_2	−22	105 (pMC)	–
DIC (end member A)	−15	105	3
DIC (end member O)	−8	60	11
DIC (end member C)	−9	0	9

In this water limited environment, when groundwater recharge occurs after a river flood event such as what was seen in March 2012, we propose that end-member A has evolved from river water (RW). The solid black arrows in Fig. 4 from RW to A represent the geochemical evolution. This groundwater end-member (A) is expected to be similar to river water with a relatively low [DIC] and high $^{14}C_{DIC}$ value (Fig. 4II), except that it is depleted in ^{13}C compared to river water (Fig. 4I). The $\delta^{13}C_{DIC}$ of this end-member should be approximately −15.0‰ (Table 2). This value is likely to have resulted from chemical equilibrium, under

open-system conditions, between $CO_{2(g)}$ (with $\delta^{13}C = -22‰$, depicted as CO_2 in Fig. 4III) in the unsaturated zone and DIC which consists of two major carbon species in water (assuming a temperature of 20 °C):

$$DIC_{(A)} = HCO_3^- + CO_{2(aq)} \quad (1)$$

	$DIC_{(A)}$	HCO_3^-	$CO_{2(aq)}$
Mole fraction	1	x	y
$\delta^{13}C^*_{DIC}$ (‰)	−15	−13(=−22 + 9)	−23(= −22 + (−1))

where $CO_{2(aq)}$ is dissolved CO_2, subscript 'A' denotes end-member A, x and y are mole fractions of HCO_3^- and $CO_{2(aq)}$ in $DIC_{(A)}$, respectively, and '*' denotes values of the carbon species when the exchange process is at equilibrium. The mole fractions of $CO_{2(aq)}$ and HCO_3^- in $DIC_{(A)}$ can be calculated from the following:

$$x = 1 - y \quad (2)$$

$$\delta^{13}C_{DIC(A)} = -15 = -13x + -23y \quad (3)$$

The calculated mole fraction of $CO_{2(aq)}$ (y) and HCO_3^- (x) in $DIC_{(A)}$ are 0.2 and 0.8, respectively. This is comparable with the calculation of the different carbon species using the measured data of sample GW096135/1 which resulted in 0.33 and 0.63, for $CO_{2(aq)}$ and HCO_3^-, respectively (Table 1) with the remaining minor fraction consisting of CO_3^{2-}. It is acknowledged that the DIC in the groundwater and the CO_2 in the unsaturated zone is probably derived from multiple flood events that may have different geochemistry (specifically $\delta^{13}C_{DIC}$ values). But what these calculations for this event do indicate is there is an excess of dissolved CO_2 in water (ca. 20–30%) that has not reacted with carbonate minerals. This excess is consistent with the observation that there is a lack of carbonate minerals in the soil profile near the river (Sections 4.3 and 5.1). This excess of dissolved CO_2 then makes the water slightly acidic (measured pH of 6.5 for GW096135/1) and causes lower [DIC] compared to other groundwater samples in the study area. If no groundwater mixing occurs between A and other end-members, it is suggested that the groundwater will continue to evolve (e.g. to end-member O) in this water-limited environment.

Compared to end-member A, O has much higher [DIC] (11 mmol L^{-1} compared to 3 mmol L^{-1}), higher $\delta^{13}C$ value (−8‰ compared to −15‰), and lower $^{14}C_{DIC}$ value (60 pmc compared to 100 pmc) (Table 2, Fig. 4). This water is suggested to have evolved from end-member A during drought. The evolution of this end-member is important for understanding carbon evolution in water-limited environments and will be discussed in detail below.

The end-member C has a very low $^{14}C_{DIC}$ (close to 0 pmc), with a $\delta^{13}C$ value of −9‰ and [DIC] of 9 mmol L^{-1} which are between end-members A and O (Table 2, Fig. 4). The low $^{14}C_{DIC}$ values are most probably due to ^{14}C decay. The hydrochemistry of this groundwater is different to others along the transect and trace-element isotope data shows that this groundwater has either originated from outside the study area or more likely migrated upwards from the underlying Great Artesian basement aquifer (Meredith et al., 2013).

5.3. DIC evolution during drought

The groundwater samples after extended drought conditions are represented in Fig. 4 as black points (squares and triangles). The grey solid-line arrows from RW via end-member A to O represent the main geochemical evolution of river water to shallow saline groundwater (<40 m bgs) after extended drought conditions. The high [DIC] (more than three times that of end-member A, Table 2) and $\delta^{13}C_{DIC}$ of end-member O cannot be explained by a simple carbonate mineral dissolution process, because end-member A contains only 20–30% of $CO_{2(aq)}$ in DIC that can further react with carbonate (see Section 5.2).

Here we explore processes relevant to this environment based on soil $CO_{2(g)}$ measurements presented in Section 5.1 that could lead to elevated [DIC] and higher $\delta^{13}C_{DIC}$ values in groundwater. In this semi-arid zone environment, evaporation is a dominant processes, and it was found that the soil profiles experience evaporation rates of 11–15 mm yr^{-1} during drought (Meredith et al., 2015). Evaporation itself may increase [DIC], but can only cause negligible fractionation of carbon isotopes. Therefore, evaporation alone cannot explain the increased [DIC] and $\delta^{13}C_{DIC}$ values in groundwater.

Increasing water-sediment interactions were found to occur with distance from the river especially in sediments from 15 to 22 m depth as identified by higher ^7Li and ^{11}B values in groundwater (Meredith et al., 2013). It was also found that this increases with distance from the river due to the decrease in water availability and longer time periods between flooding (Meredith et al., 2015). Therefore, we consider water-sediment interaction processes that can cause (1) ion exchange on clay minerals contained within the shallow aquifer (Carroll, 1959), and (2) dissolution of calcite as a result of reduced calcium carbonate. The equation of the processes is

$$\begin{aligned} &\underbrace{Ca^{2+} + CO_3^{2-}}_{\text{lower in dissolved calcite}} + Na_2X \xrightarrow{\text{ion exchange}} \\ &\underbrace{2Na^+ + CO_3^{2-} + CaX}_{\text{newly dissolved calcite}} \xrightarrow{\text{calcite dissolution}} \\ &\underbrace{\begin{array}{c} 2Na^+ + CO_3^{2-} + CaX \\ + \\ Ca^{2+} + CO_3^{2-} \end{array}}_{\text{newly dissolved calcite}} \end{aligned} \quad (4)$$

where X is the exchange site. The removal of Ca from the water would then lower the saturation state of calcite thus allowing more calcite to dissolve. This process would explain the decrease in Ca/Cl ratios in groundwater with increase in [DIC] (Fig. 5a). As this process proceeds the groundwaters would become saturated with respect to carbonate minerals, which is what we see with increasing Cl concentration in Fig. 5b.

If this process is indeed responsible for the increased [DIC] and $\delta^{13}C_{DIC}$, to calculate the contribution of addi-

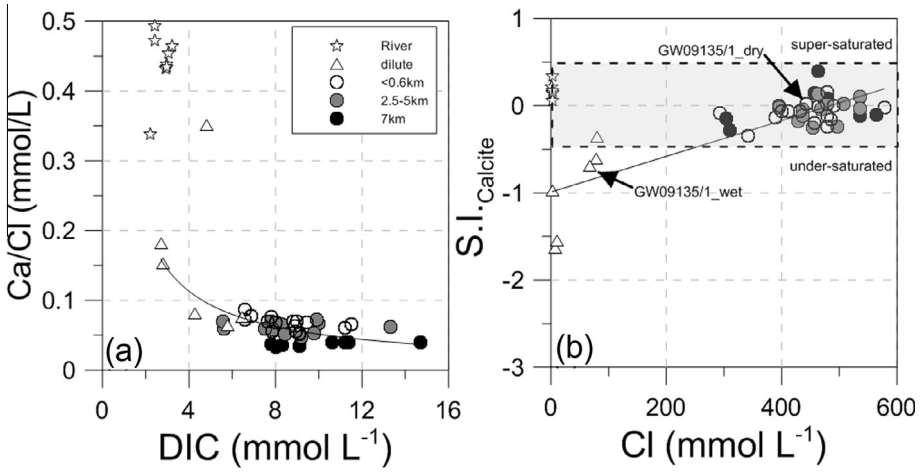

Fig. 5. Bivariate plots of (a) [DIC] vs. Ca/Cl with a power fit line ($\ln(Y) = B * \ln(X) + A$) of all groundwaters and (b) Cl^- vs. saturation index of calcite ($S.I._{calcite}$) with a linear fit line of all groundwaters ($r^2 = 0.7$). The grey shaded rectangle represents groundwaters in equilibrium with calcite.

tionally dissolved carbonate caused by ion exchange in end-member O, we ignore the concentration of $CO_{2(aq)}$, assume that the total DIC consists of two species of HCO_3^-, which is the HCO_3^- before cation exchange ($HCO_{3(before)}^-$), and the additional HCO_3^- caused by cation exchange ($HCO_{3(add)}^-$),

$$DIC_{(O)} = HCO_{3(before)}^- + HCO_{3(add)}^- \quad (5)$$

The isotopic composition of $HCO_{3(before)}^-$ can be estimated from end-member A (see the value in Eq. (3)). And the isotopic composition of $HCO_{3(add)}^-$ can be obtained by extending the solid grey arrows from A through O to the maximum value of [DIC (i.e. 1/[DIC] = 0), in sub-diagrams (I) and (II) in Fig. 4. This additional carbon source is represented by symbols 'S' (i.e. the solid carbonate value) and has $^{14}C_{DIC}$ and $\delta^{13}C_{DIC}$ values of 40 pmc and −5‰, respectively (Fig. 4I and II). Based on the $^{14}C_{DIC}$ and $\delta^{13}C_{DIC}$ values of the two mixing sources, A and S, the fraction of $HCO_{3(before)}^-(x)$ and $HCO_{3(add)}^-(y)$ can be estimated:

	$DIC_{(O)}$	$HCO_{3(before)}^-$	$HCO_{3(add)}^-$
End-member	O	A	S
Mole fraction	1	x	y
$\delta^{13}C_{DIC}$ (‰)	−8	−13	−5
$^{14}C_{DIC}$ (pmc)	60	105	40

From the following equations, fractions x and y can be calculated:

$$x = 1 - y \quad (6)$$

$$\delta^{13}C_{DIC(O)} = -13x + -5y = -8 \quad (7)$$

$$^{14}C_{DIC(O)} = 105x + 40y = 60 \quad (8)$$

The calculated y is 0.63 by using Eqs. (7) and (8), respectively. This calculation shows that more than half of the DIC in end-member O could be carbon that is added through cation exchange (fraction y) which consists of mainly dead carbon. Thus, by accounting for the additional DIC by this process, the $^{14}C_{DIC}$ value of 60 ± 10 pmc in $DIC_{(O)}$ can be attributed to dead carbon mixing, suggesting the end-member O is modern. It is not unusual for such low $^{14}C_0$ values to be derived for water-limited environments, for example Carmi et al. (2009) found a value of 54 pMC.

A binary mixing model of modern end-members A ($^{14}C_{DIC}$ = 100 pmc) and O ($^{14}C_{DIC}$ = 60 pmc) with a mixing ratio of 1:1 would result in a groundwater with $^{14}C_{DIC}$ of ca. 80 pmc. This value is consistent with ^{14}C content observations in groundwater after an extended drought period which ranged from 74 to 82 pmc suggesting that the lower $^{14}C_{DIC}$ values compared to 100 pmc is not due to ^{14}C decay but rather due to mixing of river water with geochemically evolved groundwater similar to end-member O (Fig. 6a). Tritium is only detectable in groundwaters close to the river (<0.6 km) (Table 1). This shows that groundwaters located >2.5 km are 'modern' according to the ^{14}C timescale but are not recently recharged river water (i.e. in the past 50 years). This seems reasonable if we consider large river flow events that have the potential to recharge the system occur every 20–30 years (Meredith et al., 2015). Because most samples influenced by carbonate dissolution do not contain ^3H, closed system calcite dissolution using predicted $^{14}C_{DIC}$ vs. ^3H curves (Cartwright et al., 2013) derived from the renewal rate model (Le Gal La Salle et al., 2001) was not assessed.

While ion exchange processes may be involved in the evolution of end-member O, the carbon isotopic compositions of the carbonate minerals in the unsaturated zone at 7 km from the river suggests carbon exchange between solid carbonate and DIC (i.e. the change in $^{14}C_{CaCO3}$ values in carbonates between dry and wet periods down to 2 m bgs; see Section 4.3 and Fig. 2d). Two shallow groundwater samples collected at 7 km from the river during drought (i.e. 2007) (samples GW096137/1 and GW096137/2, black solid triangles in Fig. 4) plot close to end-member O. But these samples have higher [DIC] (11.4–14.7 mmol L^{-1}) and have less negative $\delta^{13}C_{DIC}$ (−5.7 ± 0.1‰) values

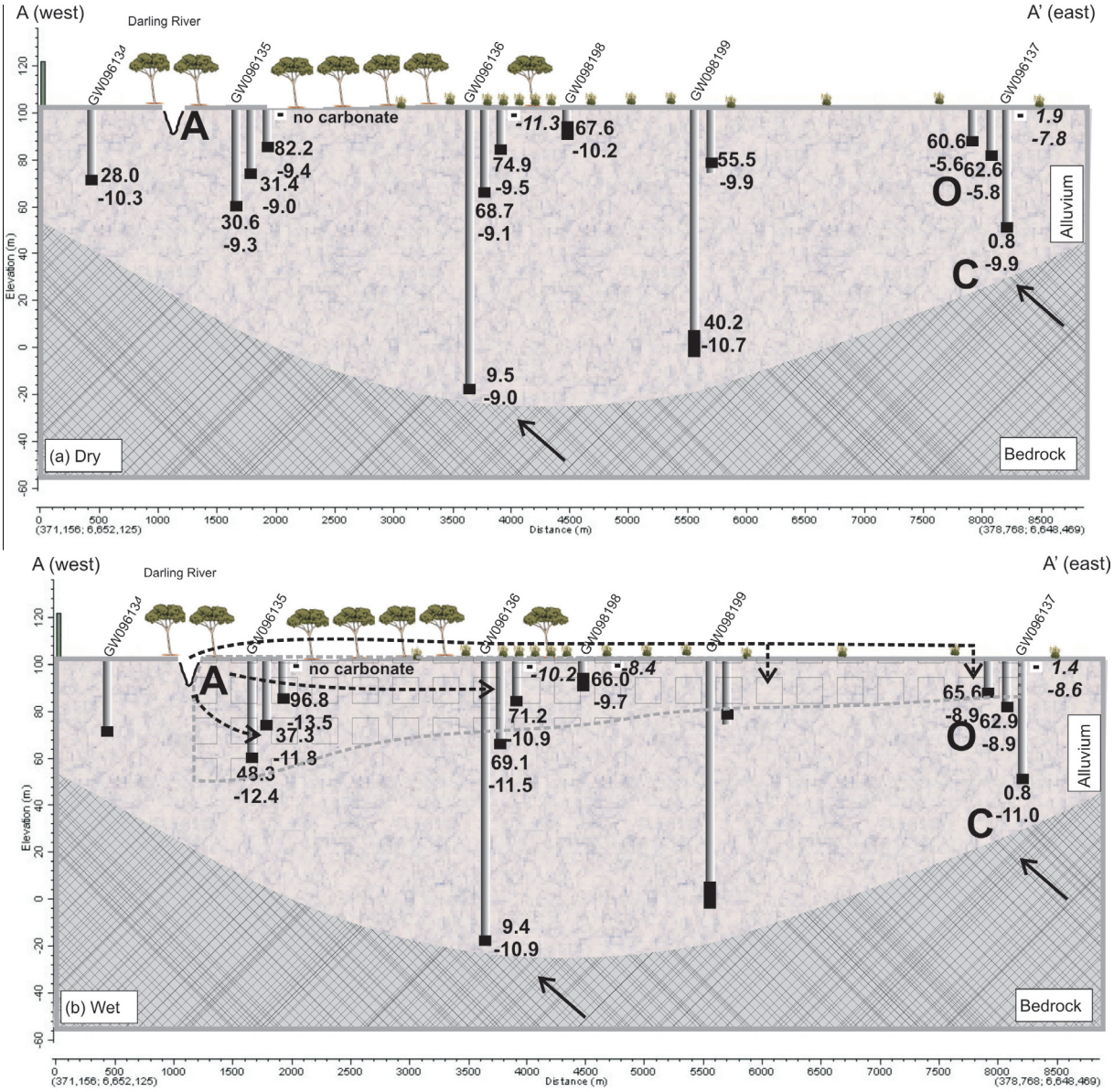

Fig. 6. Schematic cross section representation of ^{14}C (pmc i.e. positive numbers) and $\delta^{13}C$ (δ i.e. negative numbers) values for the (a) drought period (August 2007 or June 2009) and (b) post-flood (June 2012) for groundwater and carbonate minerals for cross section A (refer to Fig. 1 for cross section locations). The location of the screen intervals on the wells are depicted with dark squares. The contact and extent of the bedrock and alluvium is shown. The cross hatched polygon in (b) represents the extent of river water mixing into the aquifer post-flood (Meredith et al., 2015). The solid arrow represents the direction of regional groundwater flow forming end-member C and dotted arrows the pathways for river water recharge.

compared to other groundwaters from the study site. Thus, in addition to ion exchange, carbon exchange between solid carbonate and DIC may also be involved in the evolution of the DIC. Typically, carbon exchange between DIC and solid carbonate under closed system conditions is very slow, with the exchange rates that are comparable with the rate of ^{14}C decay (Han et al., 2014). However, repeated dissolution and precipitation of carbonate driven by drought and flood conditions could facilitate carbon exchange. For example, the following reversible process may cause carbon exchange:

$$CO_{2(aq)} + H_2O + CaCO_{3(s)} \leftrightarrow Ca^{2+} + 2HCO_3^- \quad (9)$$

In saline groundwaters such what is observed in this system (Meredith et al., 2015), the co-existence of Na^+, CO_3^{2-}, Cl^-, and Ca^{2+} in the groundwater (assuming that this solution is close to solubility equilibrium) could also facilitate carbon exchange between DIC and solid carbonate without involving CO_2. Thus, the repeated drought-flood cycles could cause carbon exchange between DIC and solid carbonate in the sediments (Myers, 2003) as observed in the top 2 m of the unsaturated zone:

$$2NaCl_{(aq)} + CaCO_{3(s)} \underset{\text{decreasing salinity}}{\overset{\text{increasing salinity}}{\rightleftharpoons}} 2Na^{+} + Ca^{2+} + 2Cl^{-} + CO_3^{2-} \underset{\text{decreasing salinity}}{\overset{\text{increasing salinity}}{\rightleftharpoons}} Na_2CO_{3(s)} + CaCl_{2(aq)} \quad (10)$$

With increasing salinity, more solid calcium carbonate tends to dissolve, and dissolved sodium carbonate tends to precipitate, and vice versa. This reversible reaction (10) does not change the chemical composition of the water and/or the sediments if drought and flooding happens periodically, and there is no net mass transfer when observed on a greater time-scale. It seems likely that a sodium carbonate would form here because a sodium bicarbonate mineral would be more likely to dehydrate and CO_2 would be released. This reversible reaction (10) will change $^{14}C_{DIC}$ and $\delta^{13}C_{DIC}$, and it would have little effect on [DIC] (see next section).

It should be noted that the two end-members A and O have similar pH values, although end-member O has evolved from A. End-member O is located away from the river, where there is ample carbonate for the dissolved CO_2 to react with solid carbonate in the unsaturated zone. Thus, end-member O would be expected to contain lower $CO_{2(aq)}$ and have a higher pH value. A possible explanation for the similar pH values is that because end-member O has a much higher salinity this will cause a lower pH value for the same $CO_{2(aq)}$ concentration.

5.4. DIC mixing after a flood event

A large flood event was observed in March 2012 resulted in approximately 1–2 m depth of flood water across the site (Meredith et al., 2015) and recharge of groundwater (Fig. 6b). After this event, the measured values of $^{14}C_{DIC}$, $\delta^{13}C_{DIC}$ and [DIC] of shallow groundwaters close to the river (<0.6 km) moved closer towards end-member A (grey triangles) and other shallow groundwaters plot along mixing line A–O (as indicated by dashed-line arrows in Fig. 4). In extreme cases (e.g. see sample GW096135/1), where the influence of river water was greatest, the groundwater evolution re-starts from end-member A. This groundwater also became fresher and moved from being in equilibrium (SI = 0) to under-saturated (SI = −0.7) with respect to calcite (Fig. 5b, Table 1). The $\delta^{13}C_{DIC}$ values become more negative for shallow groundwaters (7 km away from the river) after flooding and the DIC in groundwater is now in exchange equilibrium with the carbonate minerals contained in the sediments (c.f. $\delta^{13}C_{CaCO3}$ = −8.6‰ and $\delta^{13}C_{DIC}$ of the groundwater = −8.9‰). This $\delta^{13}C_{CaCO3}$ value of −8.6‰ is what would be expected for secondary carbonates forming from groundwater (i.e. fractionation factor of ~0.5‰ (Kalin, 1999)). Geochemical modelling (see Section 3.3) also shows that the fresh recently recharged groundwater (GW096135/1) is predicted to precipitate a carbonate with a $\delta^{13}C_{CaCO3}$ value of −8.7‰.

A comparison between the values during extended drought (Fig. 4, black squares) and after the flood event (Fig. 4, grey circles) shows that, for the deeper samples with $^{14}C_{DIC}$ less than 40 pmc located near the river (<0.6 km), mixing with river water has caused the sample points to move 'back' to the mixing line (C–A line; Fig. 4III) with more negative $\delta^{13}C_{DIC}$ values. During extended drought periods, the deeper mixed waters (containing A and C) undergo carbon exchange with carbonate minerals contained within the aquifer under closed-system conditions (Process 10). The carbon exchange process may cause an increase in $\delta^{13}C_{DIC}$ (Fig. 4III) but only little effect on [DIC] (Fig. 4I, II).

6. CONCLUSION

Estimating groundwater age is important for understanding hydrological systems. In semi-arid or water-limited environments, the complex hydrology of a catchment can mean that the groundwater may represent a mixture of waters with distinctly different ages, such as a binary mixture containing modern river water and geochemically evolved groundwater that has undergone a variety of different geochemical processes. For such water, none of the simple adjustment models for initial content of ^{14}C can be applied to provide meaningful groundwater age information, and, a more physically based definition of groundwater age is needed.

To use ^{14}C as an age indicator, an understanding of the evolution of dissolved inorganic carbon is essential. Because carbon isotopic composition of dissolved inorganic carbon ($^{14}C_{DIC}$, $\delta^{13}C_{DIC}$) is a result of many geochemical processes involving different carbon-bearing sources that may have different carbon isotopic compositions. Therefore in order to understand the evolution of DIC, the different carbon-bearing sources that may have been involved in the geochemical processes must be identified or accounted for.

In this study, together with geochemical data, we determined carbon isotope data for DIC in water, carbonate minerals in the sediments, sediment organic matter, soil gas CO_2 from the unsaturated zone, and vegetation samples. The samples were collected after an extended drought, and recollected again after a large river flood event, to capture the evolution of DIC in water after varying hydrological regimes.

A graphical method (Han et al., 2012) was applied for interpretation of the carbon geochemical and isotopic data. This method has been proved useful for analysis of the carbon geochemical and isotopic data for preliminary identification of carbon-bearing sources and geochemical processes involved in the evolution of dissolved inorganic carbon in this water-limited environment. Simple forward mass-balance modelling was carried out on major geochemical processes that had been identified by the graphical method. The results of model calculations agreed well with observed data.

This study shows that although ^{14}C cannot be applied as a dating tool in some circumstances, carbon geochemical/isotopic data can be useful in hydrological investigations related to groundwater sources, mixing relations, recharge processes, geochemical evolution, and interaction with surface water.

Further investigations are needed for this complex groundwater system because there are many uncertainties

associated with this assessment such as limited spatial coverage (especially for unsaturated zone sampling) and the assessment is based on only two monitoring events. Future investigations should involve a multi-tracer approach using dissolved noble gases for example ^{39}Ar to confirm the age of the waters that are outside the ^{3}H dating range but modern from a ^{14}C perspective, and further sediment analysis to confirm the interpretations of the carbon (isotopic and geochemical) data made in this study.

ACKNOWLEDGEMENTS

The authors would like to thank various ANSTO personnel such as Robert Chisari, Alan Williams, Fiona Bertuch, Simon Varley, Andrew Jenkinson, Barbara Gallagher and Kelly Farrawell for analysis. Thank you to Stuart Hankin, Nathan Butterworth and Chris Dimovski for their help in the field. We would also like to thank the Department of Water and Energy (Wolli Creek Laboratory) for providing groundwater data with special mention to Mike Williams and Hari Haridharan. The authors would like to especially thank Niel Plummer for reviewing an early version of the manuscript. And many thanks to Ian Cartwright and two anonymous reviewers for providing excellent suggestions that led to the significant improvement of the final manuscript. This work was funded by ANSTO Australian Nuclear Science and Technology Organisation.

REFERENCES

Allison S. D., Wallenstein M. D. and Bradford M. A. (2010) Soil-carbon response to warming dependent on microbial physiology. *Nat. Geosci.* **3**, 336–340.

Amundson R., Wang Y., Chadwick O., Trumbore S., McFadden L., McDonald E., Wells S. and DeNiro M. (1994) Factors and processes governing the ^{14}C content of carbonate in desert soils. *Earth Planet. Sci. Lett.* **125**, 385–405.

Appelo C. and Postma D. (2005) *Geochemistry, Groundwater and Pollution*, 2nd ed. A.A. Balkema, Leiden, The Netherlands, p. 649.

Carroll D. (1959) Ion exchange in clays and other minerals. *Geol. Soc. Am. Bull.* **70**, 749–779.

Carmi I., Kronfeld J., Yechieli Y., Yakir D., Boaretto E. and Stiller M. (2009) Carbon isotopes in pore water of the unsaturated zone and their relevance for initial ^{14}C activity in groundwater in the coastal aquifer of Israel. *Chem. Geol.* **268**, 189–196.

Carmi I., Yakir D., Yechieli Y., Kronfeld J. and Stiller M. (2013) Variations in soil CO_2 concentrations and isotopic values in a semi-arid region due to biotic and abiotic processes in the unsaturated zone. *Radiocarbon* **55**, 932–942.

Cartwright I. (2010) The origins and behaviour of carbon in a major semi-arid river, the Murray River, Australia, as constrained by carbon isotopes and hydrochemistry. *Appl. Geochem.* **25**, 1734–1745.

Cartwright I., Fifield K. and Morgenstern U. (2013) Using ^{3}H and ^{14}C to constrain the degree of closed-system dissolution of calcite in groundwater. *Appl. Geochem.* **32**, 118–128.

Cerling T. and Quade J. (1993) Stable carbon and oxygen isotopes in soil carbonates. Climate change in the continental isotopic records. In *Geophysical Monographs 78*. American Geophysical Union.

Cerling T. E., Solomon D. K., Quade J. and Bowman J. R. (1991) On the isotopic composition of carbon in soil carbon dioxide. *Geochim. Cosmochim. Acta* **55**, 3403–3405.

Eichinger L. (1983) A contribution to the interpretation of C-14 groundwater ages considering the example of a partially confined sandstone aquifer. *Radiocarbon* **25**, 347–356.

Fontaine S., Barot S., Barre P., Bdioui N., Mary B. and Rumpel C. (2007) Stability of organic carbon in deep soil layers controlled by fresh carbon supply. *Nature* **450**, 277–280.

Fontes J. C. and Garnier J. M. (1979) Determination of the initial ^{14}C activity of the total dissolved carbon: a review of the existing models and a new approach. *Water Resour. Res.* **15**, 399–410.

Gonfiantini R. and Zuppi G. M. (2003) Carbon isotope exchange rate of DIC in karst groundwater. *Chem. Geol.* **197**, 319–336.

Han L.-F. and Plummer L. N. (2013) Revision of Fontes & Garnier's model for the initial ^{14}C content of dissolved inorganic carbon used in groundwater dating. *Chem. Geol.* **351**, 105–114.

Han L. F. and Plummer L. N. (2016) A review of single-sample-based models and other approaches for radiocarbon dating of dissolved inorganic carbon in groundwater. *Earth Sci. Rev.* **152**, 119–142.

Han L.-F., Plummer L. N. and Aggarwal P. (2012) A graphical method to evaluate predominant geochemical processes occurring in groundwater systems for radiocarbon dating. *Chem. Geol.* **318–319**, 88–112.

Han L.-F., Niel Plummer L. and Aggarwal P. (2014) The curved ^{14}C vs. δ^{13}C relationship in dissolved inorganic carbon: a useful tool for groundwater age- and geochemical interpretations. *Chem. Geol.* **387**, 111–125.

Hua Q., Jacobsen G., Zoppi U., Lawson E., Williams A., Smith A. and McGann M. (2001) Progress in radiocarbon target preparation at the ANTARES AMS Centre. *Radiocarbon* **43**, 275–282.

Kalin R. M. (1999) Radiocarbon dating of groundwater systems. In *Environmental Tracers in Subsurface Hydrology* (eds. P. G. Cook and A. L. Herczeg). Kluwer Academic Publishers, New York, pp. 111–144.

Le Gal La Salle C., Marlin C., Leduc C., Taupin J. D., Massault M. and Favreau G. (2001) Renewal rate estimation of groundwater based on radioactive tracers (^{3}H, ^{14}C) in an unconfined aquifer in a semi-arid area, Iullemeden Basin. *Niger. J. Hydrol.* **254**, 145–156.

Longnecker K. and Kujawinski E. B. (2011) Composition of dissolved organic matter in groundwater. *Geochim. Cosmochim. Acta* **75**, 2752–2761.

Maloszewski P. and Zuber A. (1991) Influence of matrix diffusion and exchange reactions on radiocarbon ages in fissured carbonate aquifers. *Water Resour. Res.* **27**, 1937–1945.

Mattey D. P., Atkinson T. C., Barker J. A., Fisher R., Latin J. P., Durell R. and Ainsworth M. (2016) Carbon dioxide, ground air and carbon cycling in Gibraltar karst. *Geochim. Cosmochim. Acta* **184**, 88–113.

Meredith K. T., Hollins S. E., Hughes C. E., Cendón D. I., Hankin S. and Stone D. J. M. (2009) Temporal variation in stable isotopes (^{18}O and ^{2}H) and major ion concentrations within the Darling River between Bourke and Wilcannia due to variable flows, saline groundwater influx and evaporation. *J. Hydrol.* **378**, 313–324.

Mazumder D., Iles J., Kelleway J., Kobayashi T., Knowles L., Saintilan N. and Hollins S. (2010) Effect of acidification on elemental and isotopic compositions of sediment organic matter and macro-invertebrate muscle tissues in food web research. *Rapid Commun. Mass Spectrom.* **24**, 2938–2942.

Meredith K., Cendón D. I., Pigois J.-P., Hollins S. and Jacobsen G. (2012) Using ^{14}C and ^{3}H to delineate a recharge 'window' into the Perth Basin aquifers, North Gnangara groundwater system, Western Australia. *Sci. Total Environ.* **414**, 456–469.

Meredith K., Moriguti T., Tomascak P., Hollins S. and Nakamura E. (2013) The lithium, boron and strontium isotopic systematics of groundwaters from an arid aquifer system: implications for recharge and weathering processes. *Geochim. Cosmochim. Acta* **112**, 20–31.

Meredith K. T., Hollins S. E., Hughes C. E., Cendón D. I., Chisari R., Griffiths A. and Crawford J. (2015) Evaporation and concentration gradients created by episodic river recharge in a semi-arid zone aquifer: Insights from Cl^-, $\delta^{18}O$, δ^2H, and ^3H. 529. *J. Hydrol.* **529**(Part 3), 1070–1078.

Mook W. G. (1976) The dissolution-exchange model for dating groundwater with ^{14}C. In *Interpretation of Environmental Isotope and Hydrochemical Data in Groundwater Hydrology*, Vienna.

Mook W. (1980) Carbon-14 in hydrogeological studies. In *Handbook of Environmental Isotopes Geochemistry*, Vol. 1 (eds. P. Fritz and J. C. Fontes). Elsevier, Amsterdam, pp. 49–74.

Myers R. (2003) *Basics of Chemistry*. Greenwood Publishing Group, p. 373.

Parkhurst D. and Appelo C. (1999) User's guide to PHREEQC (version 2) – a computer program for speciation, batch-reaction, one dimensional transport, and inverse geochemical calculations. In *USGS Water Resources Investigations Report 99*, 4259.

Plummer L. N. (1977) Defining reactions and mass transfer in part of the Floridan aquifer. *Water Resour. Res.* **13**, 801–812.

Plummer L. N. and Glynn P. D. (2013) Radiocarbon dating in groundwater systems. In *IAEA, 2013, Isotope Methods for Dating Old Groundwater*. International Atomic Energy Agency, Vienna, p. 357. April, 2013, Chap. 4, 3–89. STI/PUB/1587, ISBN 978–92–0–137210–9, http://www-pub.iaea.org/books/IAEABooks/8880/Isotope-Methods-for-Dating-Old-Groundwater.

Plummer N. and Sprinkle C. (2001) Radiocarbon dating of dissolved inorganic carbon in groundwater from confined parts of the Upper Floridan aquifer, Florida, USA. *Hydrogeol. J.* **9**, 127–150.

Quinton J. N., Govers G., Van Oost K. and Bardgett R. D. (2010) The impact of agricultural soil erosion on biogeochemical cycling. *Nat. Geosci.* **3**, 311–314.

Salem O., Visser J. H., Dray M. and Gonfiantini R. (1980) Groundwater flow patterns in the western Lybian Arab Jamahiriaya. In *Arid-zone Hydrology: Investigations with Isotope Techniques*. IAEA, Vienna, pp. 165–179.

Sanford W. (1997) Correcting for diffusion in carbon-14 dating of ground water. *Ground Water* **35**, 357–361.

Shen Y., Chapelle F., Strom E. and Benner R. (2015) Origins and bioavailability of dissolved organic matter in groundwater. *Biogeochemistry* **122**, 61–78.

Tadros C. V., Hughes C. E., Crawford J., Hollins S. E. and Chisari R. (2014) Tritium in Australian precipitation: a 50 year record. *J. Hydrol.* **513**, 262–273.

Tamers M. A. (1975) Validity of radiocarbon dates on ground water. *Geophys. Surv.* **2**, 217–239.

Walvoord M. A., Striegl R. G., Prudic D. E. and Stonestrom D. A. (2005) CO_2 dynamics in the Amargosa Desert: fluxes and isotopic speciation in a deep unsaturated zone. *Water Res. Res.* **41**, n/a-n/a.

Wigley T. M. L., Plummer L. N. and Pearson F. J. J. (1978) Mass transfer and carbon isotope evolution in natural water systems. *Geochim. Cosmochim. Acta* **42**(42), 1117–1139.

Wood C., Cook P. G., Harrington G. A., Meredith K. and Kipfer R. (2014) Factors affecting carbon-14 activity of unsaturated zone CO_2 and implications for groundwater dating. *J. Hydrol.* **519**, 465–475.

Associate editor: Orit Sivan